Proton Spin Relaxation in Reentrant Nematic Cyano-biphenyl Liquid Crystals

K. H. Schweikert and F. Noack

Physikalisches Institut der Universität Stuttgart, Stuttgart, FRG

Z. Naturforsch. **44a,** 597–609 (1989); received April 19, 1989

The frequency dependence of the longitudinal proton spin relaxation time T_1 was measured by field-cycling and standard NMR techniques in the nematic, smectic and reentrant nematic mesophases of the reentrant liquid crystal 6OCB–8OCB. The results clearly demonstrate that, in contrast to conclusions reported in the literature, the underlying relaxation mechanisms are the same for the nematic and reentrant nematic order, but different in the nematic and smectic phase. In particular, at low frequencies the nematic and reentrant samples reveal a square-root dispersion profile ($T_1 \sim \nu^{1/2}$) characteristic for nematic director fluctuations, whereas the smectic samples show a dissimilar and only very narrow dispersion step. It can be attributed to a linear relaxation time increase ($T_1 \sim \nu^1$) expected for smectic-type order fluctuations. The experimental data are described and discussed in terms of four molecular processes, namely nematic or smectic order fluctuations, self-diffusion, rotational motions, and a resonant proton nitrogen coupling.

Key words: Spin relaxation, Field-cycling, Liquid crystals, Reentrant nematic.

1. The Problem

In a series of papers Dong et al. [1–6] and more recently Miyajima et al. [7, 8] presented and analysed NMR relaxation measurements of liquid crystals which exhibit a reentrant nematic phase [9], i.e. a nematic ordering at temperatures lower than the stability range of a higher order smectic state. Essentially, the aim was to study possible distinctions between the molecular reorientations of the normal "high-temperature" nematic and the unusual "low-temperature" reentrant nematic mesophase, because little is known about the dynamical molecular properties. The phenomenon of reentrance has been observed for quite a number of mesogenic compounds [9, 10] and is more or less quantitatively explained by a strong antiparallel correlation between two neighbouring rodlike molecules [9–13]. Such a correlation is supposed to entail the organization of dimers which are bulgy in the middle of the pair, and by this geometry destabilize with increasing concentration the smectic layer structure in favour of a non-layered nematic-type structure. On the time scale of X-ray experiments this concept of dimer formation seems well-established [14]. However, the available X-ray measurements do not allow conclusions about the involved dynamical behaviour, for instance about the reorientation or life times of the dimers in comparison to the motions of individual rods in a nematic potential.

By considering measurements of the longitudinal proton spin relaxation rate $1/T_1$ in a well-known reentrant mesogenic alloy [15], namely a mixture of octyloxycyanobiphenyl (8OCB) and hexyloxycyanobiphenyl (6OCB), Dong concluded that in this case quite different mechanisms are responsible for the relaxation observed in the reentrant and normal nematic phase, respectively: On the one hand order fluctuations (OF) of the director field in the low-temperature state, and on the other hand self-diffusion (SD) in the high-temperature state. Furthermore, the experimental data for the intermediate smectic phase were found compatible with a superposition of both types of relaxation contributions. This circumstance, and some parallels to the temperature dependence of the viscosity of the system finally led to the result that the different properties of T_1 essentially originate from temperature induced viscosity changes, which shift the importance of the two mechanisms. In other words, novel effects typical for reentrants and absent in proper nematics were not found [1–6]. At least qualitatively, Miyajima [7, 8] observed a similar behaviour of the proton spin relaxation rate in the one-component

---

Reprint requests to Prof. Dr. F. Noack, Physikalisches Institut der Universität Stuttgart, Pfaffenwaldring 57, 7000 Stuttgart 80, FRG.

0932-0784 / 89 / 0700-0597 $ 01.30/0. – Please order a reprint rather than making your own copy.

reentrant liquid crystal octyloxybenzoyloxybenzylidene-cyanoaniline (OBBC), however surprisingly with the OF mechanism in this case governing the high-temperature and the SD mechanism dominant in the low-temperature nematic phase.

To appreciate the meaning of these findings one should realize that, through the availability and application of fast field-cycling NMR techniques [16, 17] to investigate molecular reorientations in liquid crystals, it has been demonstrated for numerous non-reentrant mesogens [18–22] that relaxation measurements by means of standard NMR spectrometers, which operate at Larmor frequencies in the megahertz range, were generally wrongly interpreted concerning the importance of order fluctuations. In any case, where field-cycling studies are available, the characteristic effects of collective molecular motions on the relaxation process have been detected only on a much slower frequency scale, namely at Larmor frequencies in the kilohertz regime! Hence, to allow a more reliable analysis of the dynamics in reentrant systems, we have extended Dong's work on 6OCB–8OCB mixtures to significantly lower frequencies using the field-cycling apparatus developed in our laboratory [23–25]. To a large extent it eliminates the sensitivity problems of standard NMR in weak Zeeman fields [16, 17].

2. Experimental Techniques and Results

2.1. Sample Preparation

According to Cladis et al. [10, 15], mixtures of hexyloxycyanobiphenyl (6OCB) and octyloxycyanobiphenyl (8OCB) with more than 22 wt.% but less than 29 wt.% of 6OCB show, in addition to the nematic and smectic liquid crystalline phases, a reentrant nematic mesophase. We prepared a sample with 27 wt.% 6OCB, because such a mixture was also studied by Dong. One should note that the stability range of the reentrant state as a function of temperature increases with higher concentration of the shorter 6OCB molecules, whereas the smectic range decreases. For this reason the selected mixture has comparable widths of the two temperature intervals above and below the phase transition. The pure compounds 6OCB and 8OCB were obtained from BDH Chemicals Ltd. and mixed with an accuracy of better than 0.5 wt.% by weighing. Relaxation measurements in different Zeeman fields with the help of field-cycling methods require only one single sample size, namely for our spectrometers approximately 1 cm^3 in glass tubes with a diameter of 1 cm. After filling the tubes, the samples were degassed by the usual freeze-pump-thaw technique and then sealed under vacuum. No degradation effects could be observed over several months. Changes of the phase transition temperature would have been easily detectable through the related variations of the NMR free induction decay signal.

2.2. NMR Apparatus

The longitudinal proton relaxation time T_1 of the described 6OCB–8OCB alloy was studied as a function of Larmor frequency $\nu \equiv \omega/2\pi$ (300 Hz $\leqq \nu \leqq 68$ MHz) and temperature ϑ (25 °C $\leqq \vartheta \leqq$ 85 °C) by means of two complementary instruments: Between 300 Hz and 7 MHz using mainly one of our homebuilt fast field-cycling devices [23], and for the higher frequencies using a standard frequency variable pulsed spectrometer [23]. Details about the underlying procedures and pulse programs, in particular on the performance of field-cycling, have been described previously [16, 17]. Some improvements were added to better control the adiabaticity and the earth's field compensation of the switching network [26].

As a rule, the random error of the computer assisted T_1 evaluation could be reduced to less than $\pm 5\%$ by averaging both the signal amplitudes and the magnetization decays up to 10 times. For reasons not yet fully understood, and regardless of the aforementioned modifications, the experimental scatter always notably rose at frequencies lower than about 5 kHz, so that more data had to be averaged. In comparison with T_1 the inaccuracy of both ν and ϑ is almost negligible. The observed relaxation process was found purely exponential over at least two time constants in all the mesophases of the mixture. To avoid undesired effects due to different orientations of the director axis relative to the applied magnetic field, any measurement was started by heating the sample to the isotropic phase and then adjusting a selected temperature under the action of the maximum flux density available in the spectrometers. In addition, the nematic-isotropic transition, which dramatically changes the form of the free induction decay signal, allowed to examine the stability and the gradient of the temperature regulation. The fluctuations turned out to be less than 0.5 °C/h and 0.5 °C/cm, respectively.

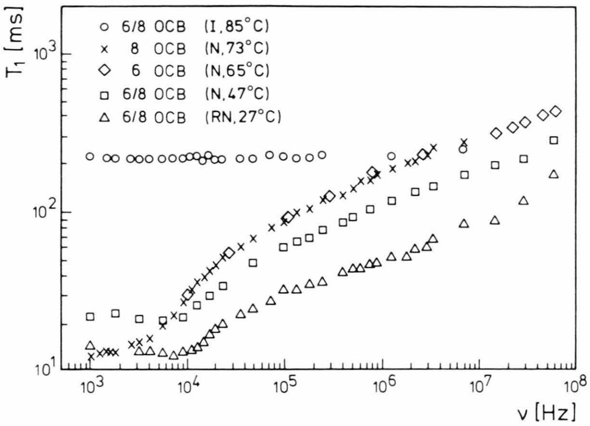

Fig. 1. Frequency dependence of the proton spin relaxation time T_1 in the isotropic, nematic and reentrant nematic phase of a 6OCB–8OCB liquid crystal alloy (27:73 wt.%). Measurements for the pure components 6OCB and 8OCB are shown for comparison.

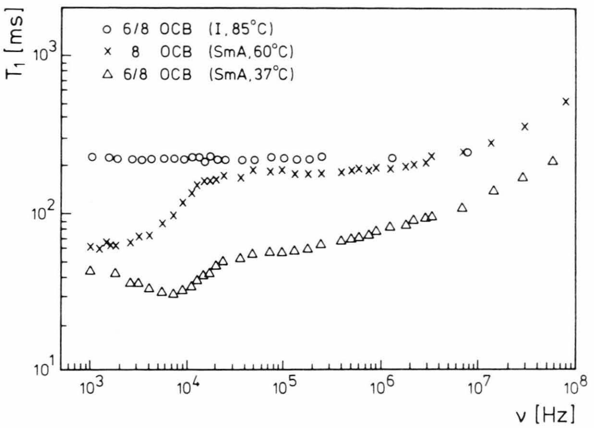

Fig. 2. Frequency dependence of the proton spin relaxation time T_1 in the isotropic and smectic phase of a 6OCB–8OCB liquid crystal alloy (27:73 wt.%). Measurements for the pure component 8OCB are shown for comparison.

2.3. *Frequency and Temperature Dependent Measurements*

Figures 1 and 2 illustrate our $T_1(\nu)$ results for the various mesophases and the isotropic state of the liquid crystal alloy. For clarity, the nematic and smectic dispersion profiles are shown separately. Both diagrams include data of the pure compounds 6OCB and 8OCB, which do not have a reentrant phase. Dispersion measurements were performed at temperatures approximately in the middle of the individual mesophases, and also near the transitions; but only a selection is represented because the variations are relatively small. As seen in Fig. 3 for some selected high and low Larmor frequencies, the maximum $T_1(\vartheta)$ change in the nematic, smectic or reentrant state is less than a factor of two. Finally we note that Dong's proton T_1 measurements in the megahertz regime [1–3] are essentially confirmed within the experimental error limits.

A qualitative inspection of the $T_1(\nu)$ and $T_1(\vartheta)$ data reveals some characteristic properties and systematic distinctions, which lay the foundation for the following quantitative analysis.

(a) The relaxation dispersion differs significantly between the nematic and smectic phases. Though it looks similar at very low frequencies and for very high frequencies, in the nematic case (Fig. 1) there exists a $T_1 \sim \nu^{1/2}$ regime between $20\,\mathrm{kHz} \lesssim \nu \lesssim 200\,\mathrm{kHz}$, which is absent in the smectic case (Fig. 2), where $T_1(\nu)$ begins to develop a plateau.

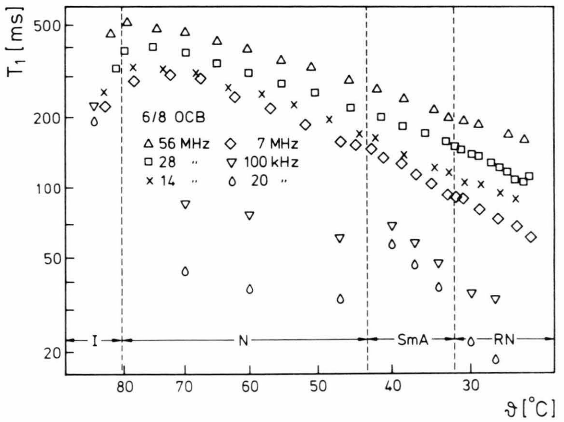

Fig. 3. Temperature dependence of the proton spin relaxation time T_1 in the isotropic, nematic, smectic and reentrant nematic phase of a 6OCB–8OCB liquid crystal alloy (27:73 wt.%) at selected Larmor frequencies in the high, medium and low field range.

(b) The results for the normal nematic and reentrant nematic sample do not differ basically. In addition to the $T_1 \sim \nu^{1/2}$ range, one observes in both cases a plateau on the low-frequency side and a transition to another shallow dispersion profile on the high-frequency side, a behaviour well-known for a great variety of nematics.

(c) The transition from the normal nematic to the smectic phase shortens the relaxation times at high Larmor frequencies and lengthens them at low frequenices, so that the total smectic dispersion step is relatively small. Taking this finding into account, the smectic profiles below $\nu \approx 20$ kHz reflect a contribution to T_1 with a dispersion significantly stronger than a square-root law, namely approximately a linear relationship $T_1 \sim \nu^1$, as most clearly seen from the pure 8 OCB sample.

(d) All dispersion diagrams have in common that the low- and high-frequency dispersion separates at least two kinds of underlying processes. This is not only indicated by the changing slopes of the $T_1(\nu)$ and $T_1(1/\vartheta)$ plots, but also and even better by comparison with the measurements in the isotropic phase, where the slow process completely disappears.

(e) The dispersion of the mixture in the nematic, smectic and reentrant phase reveals an effect not, or not clearly, seen for the pure compounds, namely a shallow $T_1(\nu)$ minimum near 10^4 Hz. The dip is superimposed on the nematic $T_1 \sim \nu^{1/2}$ and smectic $T_1 \sim \nu^1$ profile, and thus somewhat conceals the true exponent of the dominating dispersion law.

In view of these rich phenomena the high-field NMR experiments reported in the literature [1–8] do not give detailed informations on the distinctions between the three mesophases and hence have to be reinterpreted. We learn from the new results that a quantitative model for T_1 in nematic reentrants has to consider molecular mechanisms rather similar to the ones used in previous works for normal nematics [18–22]. In particular, (a) and (b) suggest through the square-root law range that in the reentrant state nematic-like and not smectic-like order fluctuations dominate the low-field relaxation [27–29]. In contrast to this, (c) gives evidence of a smectic-type relaxation contribution above the reentrant-smectic transition temperature through the linear frequency dependence [29]. Furthermore, (d) illustrates that the high-field process is similar in both the liquid crystalline and the isotropic phases. Such a behaviour has previously been ascribed to reorientations of individual molecules, namely translational [30, 31] and rotational [32, 33] diffusion because of the broad dispersion range involved in this superposition. Finally, (e) shows that the novel T_1 contribution which modifies the familiar linear or square-root low-field dispersion is inherent to the mixture and not to the reentrant, so that an explanation has to look for special geometric rather than general mesophase effects.

Hence to analyse the new reentrant data quantitatively we follow, as far as possible, the concepts developed for proton relaxation in nematic liquid crystals [18–22], and then contrast our calculations with predictions based on a model with smectic order fluctuations [34–37].

3. Discussion

3.1. Relaxation Model and Curve Fittings

As mentioned before, it has been observed in numerous field-cycling studies of mesogens that on the on hand the relaxation dispersion of nematic phases [18–22] can be understood in terms of nematic order fluctuations of the director ($\mathrm{OF}_{\mathrm{nem}}$, damped modes propagating in three directions, $T_1 \sim \nu^{1/2}$), nearly isotropical translational self-diffusion (SD), and anisotropical molecular rotations about special axes (R). On the other hand most of the dispersion profiles reported for smectic phases [34–37], typically a strong increase at low Larmor frequencies followed by a plateau and then by another, yet smaller growth at high Larmor frequencies, have been attributed to a combination of smectic order fluctuations of the director ($\mathrm{OF}_{\mathrm{sm}}$, damped modes propagating in the layer planes, $T_1 \sim \nu^1$) with self-diffusion and anisotropical rotations similar to nematics, though some details are less clear. Due to the occurrence of a $T_1(\nu)$ minimum in the mixture, these concepts are insufficient to describe the present experimental data, since none of the classical contributions can explain such a dip. As a first approach to correct the available models, we introduce a fourth relaxation process which entails the spectacular minimum, namely a term with a Lorentzian intensity spectrum (L) of the underlying molecular reorientation [16, 17, 38]. It can have different origins that will be discussed in the next section.

By means of computer assisted curve fitting techniques [19, 26, 27] it proved possible to describe all the measurements, i.e. for both the pure compounds and the mixture, by a combination of the designated mechanisms ($\mathrm{OF}_{\mathrm{nem}}$, $\mathrm{OF}_{\mathrm{sm}}$, SD, R, L) and by appropriate adjustments of their individual strengths. Details of the considered theoretical model

$$\frac{1}{T_1(\nu, \vartheta)} = \frac{1}{T_{1\,\mathrm{OF}(i)}} + \frac{1}{T_{1\mathrm{SD}}} + \frac{1}{T_{1\mathrm{R}}} + \frac{1}{R_{1\mathrm{L}}}, \quad (1)$$

where the subscripts distinguish the different reorientation processes with either $(i) = \mathrm{nem}$ or $(i) = \mathrm{sm}$, were taken from the literature [27–33, 38–46] and are summarized in Table 1 for further reference. The formulae show that each term can be characterized by an amplitude factor ($A_{(i)}$, B, C or E), by a spectral function

Table 1. Model relations used in the curve fitting of (2) to the relaxation dispersion measurements of a nematic, smectic and reentrant nematic 6OCB–8OCB mixture shown in Figs. 1 and 2. The special notation of molecular and liquid crystal properties essentially follows the original papers and is explained in the text. As usual, μ_0 is the magnetic permeability of vacuum, $\hbar \equiv h/2\pi$ Planck's constant divided by 2π, k Boltzmann's constant, γ the proton magnetogyric ratio, $\nu \equiv \omega/2\pi$ the proton Larmor frequency, and ϑ the absolute temperature in SI units.

Reorientation process	Relaxation rate	Ref.
Nematic order fluctuations (director modes)	$\frac{1}{T_{1\mathrm{OF\,nem}}} = \frac{A_{\mathrm{nem}}}{\nu^{1/2}}\left[1 - \frac{1}{\pi}\left[\mathrm{arctg}\left[(2\nu/\nu_c)^{1/2}/(\nu/\nu_c - 1)\right] - \mathrm{artgh}\left[(2\nu/\nu_c)^{1/2}/(\nu/\nu_c + 1)\right]\right]\right] + \Theta(\nu/\nu_c - 1);$	[40, 43, 45]
	$A_{\mathrm{nem}} = \left[\frac{\mu_0}{4\pi}\right]^2 \frac{9}{8}\gamma^4 \hbar^2 \frac{k\,\vartheta\,\eta^{1/2} S^2}{\pi^{1/2} K^{3/2}} \frac{(3\cos^2\varphi - 1)^2}{4a^6}, \quad \nu_c \cong \frac{2\pi}{\xi^2}\frac{K}{\eta}.$	
Smectic order fluctuations (undulation modes)	$\frac{1}{T_{1\mathrm{OF\,sm}}} = \frac{A_{\mathrm{sm}}}{\nu}\left[1 - \frac{2}{\pi}\mathrm{arctg}(\nu_c/\nu)\right];$	[36, 46]
	$A_{\mathrm{sm}} = \left[\frac{\mu_0}{4\pi}\right]^2 \frac{9}{8}\gamma^4 \hbar^2 \frac{k\,\vartheta\,S^2}{4K\,\xi} \frac{(3\cos^2\varphi - 1)^2}{4a^6}, \quad \nu_c \cong \frac{2\pi}{\xi^2}\frac{K}{\eta}.$	
Self-diffusion (isotropic approximation)	$\frac{1}{T_{1\mathrm{SD}}} = B\,\tau_{\mathrm{SD}} \sum_{p=1}^{2} p^2 \frac{\tau_{\mathrm{SD}}}{x^4}\left[\frac{x}{2} - \frac{1}{x} + e^{-x}\left(\left[\frac{x}{2} - \frac{1}{x}\right]\sin x + \left[\frac{x}{2} + \frac{1}{x} + 2\right]\cos x\right)\right];$	[31, 38]
	$B = \left[\frac{\mu_0}{4\pi}\right]^2 \frac{9}{8}\gamma^4 \hbar^2 \frac{32\pi N}{d^3}, \quad x \equiv (p\,12\pi\,\nu\,\tau_{\mathrm{SD}})^{1/2}.$	
Rotation (isotropic approximation)	$\frac{1}{T_{1\mathrm{R}}} = C\,\tau_{\mathrm{R}} \sum_{p=1}^{2} p^2 \frac{1}{1 + (p\,2\pi\,\nu\,\tau_{\mathrm{R}})^2}; \quad C = \left[\frac{\mu_0}{4\pi}\right]^2 \frac{9}{8}\gamma^4 \hbar^2 \frac{1}{15 b^6}.$	[38]
Lorentz spectrum (level crossing)	$\frac{1}{T_{1\mathrm{L}}} = E\,\tau_{\mathrm{L}} \sum_{p=-1}^{2} p^2 \frac{1}{1 + (p\,2\pi(\nu - \nu_{\mathrm{L}})\,\tau_{\mathrm{L}})^2}; \quad E = f(K_{\mathrm{Q}}, \eta_{\mathrm{Q}}, \gamma).$	[38, 65, 67]

($f_{\mathrm{OF}(i)}$, f_{SD}, f_{R} or f_{L}), and by a typical time constant ($\tau_{\mathrm{OF}(i)}$, τ_{SD}, τ_{R} or τ_{L}). In addition, the Lorentzian spectrum introduces a resonance frequency (ν_{L}), which determines the position of the T_1 versus ν minimum. One should note that sometimes the model parameter $\tau_{\mathrm{OF}(i)}$ is replaced by the related cut-off frequency of the director modes, $\nu_c = 1/(2\pi\,\tau_{\mathrm{OF}})$ [40, 43], but this obviously conceals the analogies between the various relaxation contributions. Making use of the specified general notation we write (1) more explicitly as two alternative combinations applicable to either the nematic or the smectic samples, namely [26]

$$1/T_1 = A_{(i)}\,\nu^{\alpha} f_{\mathrm{OF}(i)}(\nu, \tau_{\mathrm{OF}(i)}) + B\,\tau_{\mathrm{SD}}\,f_{\mathrm{SD}}(\nu, \tau_{\mathrm{SD}}) + C\,\tau_{\mathrm{R}}\,f_{\mathrm{R}}(\nu, \tau_{\mathrm{R}}) + E\,\tau_{\mathrm{L}}\,f_{\mathrm{L}}(\nu, \tau_{\mathrm{L}}, \nu_{\mathrm{L}}), \tag{2}$$

with $\alpha = -1/2$ for (i) = nem and $\alpha = -1$ for (i) = sm. The linear dependence of $1/T_1$ on the reorientation times τ_{SD}, τ_{R}, and τ_{L} is separated from the related spectral functions, because it allows a more expedient normalization of the frequency dependence and in this way a more convenient computer handling.

Equation (2) involves 9 unknown parameters! In order to demonstrate how relaxation dispersion measurements over a broad Larmor frequency range make possible to analyse a motional model with so many variables, Figs. 4 and 5 illustrate the fitting procedure to the experimental $T_1(\nu)$ data for the reentrant and smectic phase of the 6OCB–8OCB mixture in three steps, which successively take into account an increasing number of mechanisms. It turns out that,

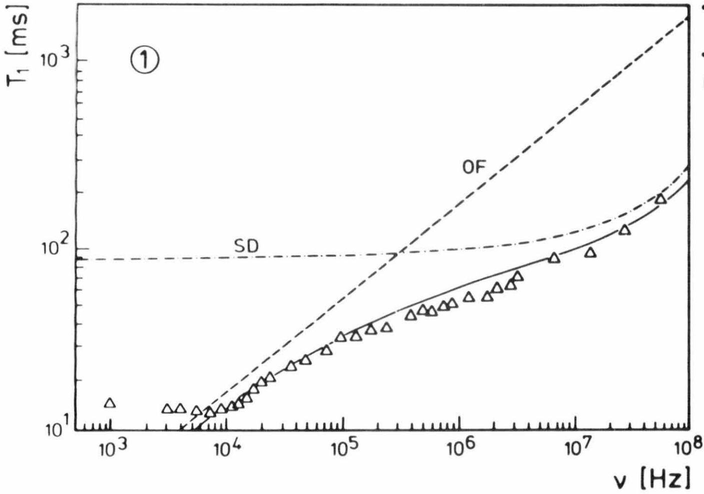

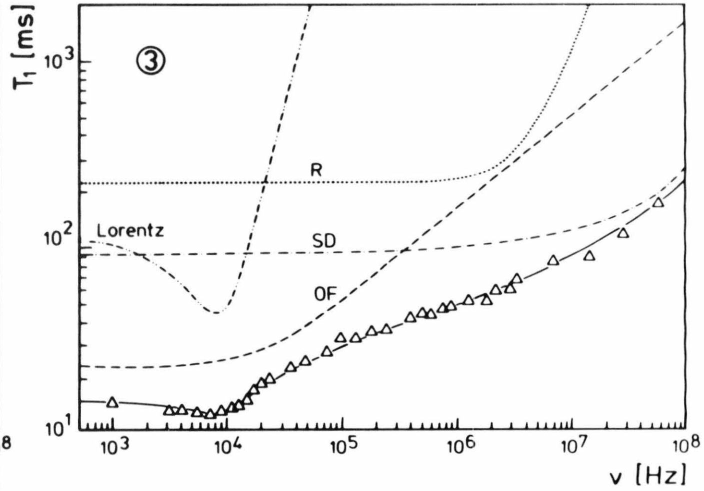

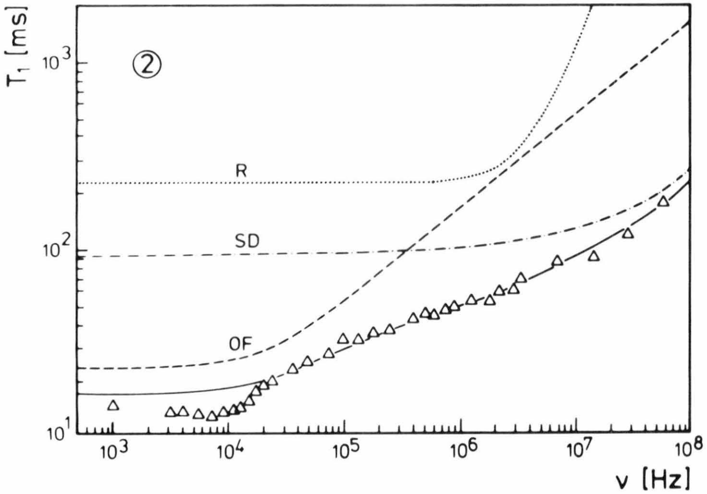

Fig. 4. Model fitting of (2) (details see Table 1) to the relaxation dispersion measurements of a reentrant nematic 6OCB–8OCB mixture shown in Figure 1. The optimized model parameters are listed in Table 2.

6OCB–8OCB (27:73 wt.%, RN, 27 °C)

Step ① $$\frac{1}{T_1}=\frac{1}{T_{1\mathrm{OF}}}+\frac{1}{T_{1\mathrm{SD}}},$$

Step ② $$\frac{1}{T_1}=\frac{1}{T_{1\mathrm{OF}}}+\frac{1}{T_{1\mathrm{SD}}}+\frac{1}{T_{1\mathrm{R}}},$$

Step ③ $$\frac{1}{T_1}=\frac{1}{T_{1\mathrm{OF}}}+\frac{1}{T_{1\mathrm{SD}}}+\frac{1}{T_{1\mathrm{R}}}+\frac{1}{T_{1\mathrm{L}}}.$$

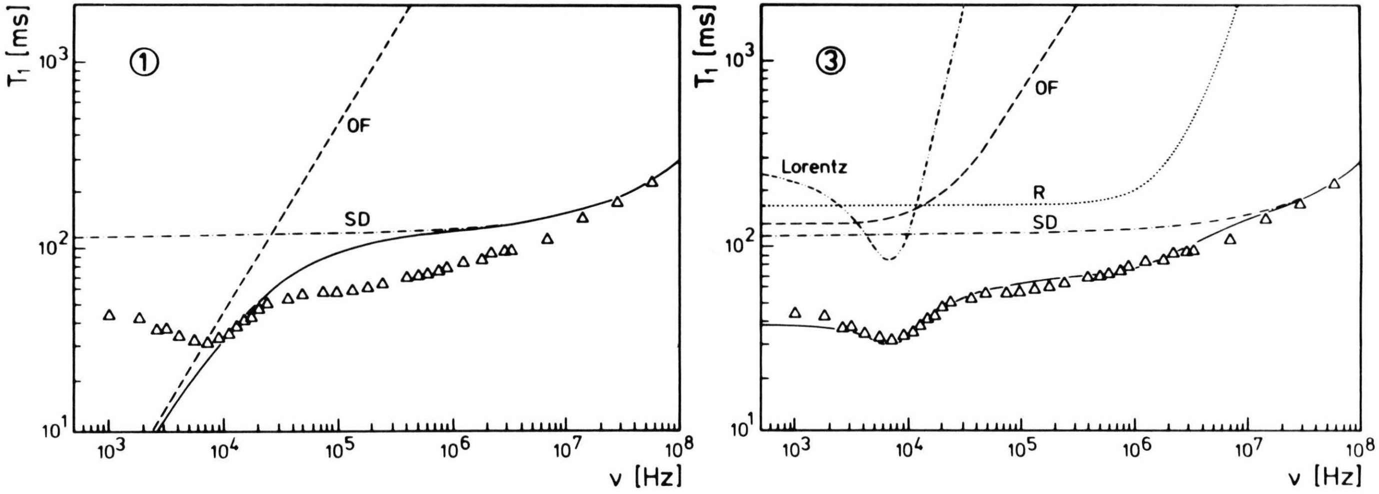

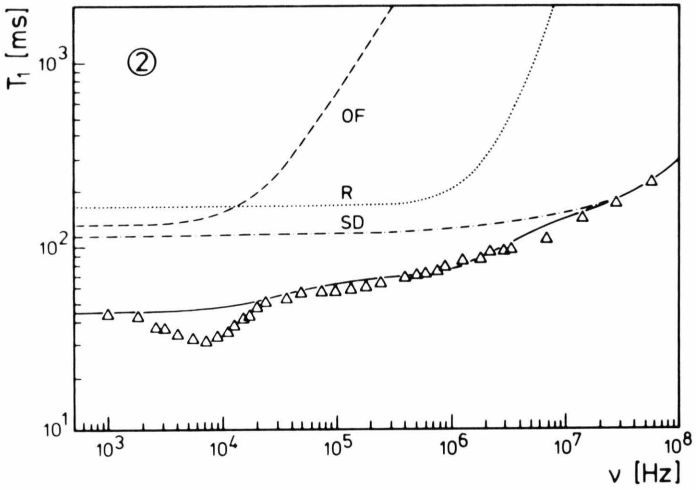

Fig. 5. Model fitting of (2) (details see Table 1) to the relaxation dispersion measurements of a smectic 6OCB–8OCB mixture shown in Figure 2. The optimized model parameters are listed in Table 2.

6OCB–8OCB (27:73 wt.%, Sm, 37 °C)

Step ① $$\frac{1}{T_1} = \frac{1}{T_{1\mathrm{OF}}} + \frac{1}{T_{1\mathrm{SD}}},$$

Step ② $$\frac{1}{T_{1\mathrm{OF}}} = \frac{1}{T_{1\mathrm{OF}}} + \frac{1}{T_{1\mathrm{SD}}} + \frac{1}{T_{1\mathrm{R}}},$$

Step ③ $$\frac{1}{T_1} = \frac{1}{T_{1\mathrm{OF}}} + \frac{1}{T_{1\mathrm{SD}}} + \frac{1}{T_{1\mathrm{R}}} + \frac{1}{T_{1\mathrm{L}}}.$$

Table 2. Optimized model parameters of the individual relaxation contributions in (2) (details see Table 1) obtained by the curve fitting to the relaxation dispersion in the three liquid crystalline mesophases of a 6OCB–8OCB mixture with a reentrant regime (27:73 wt.%).

Meso-phase	$\frac{A_{\text{nem}}}{\text{s}^{-3/2}}$	$\frac{A_{\text{sm}}}{\text{s}^{-2}}$	$\frac{\nu_c}{\text{Hz}}$	$\frac{B}{\text{s}^{-2}}$	$\frac{\tau_{\text{SD}}}{\text{s}}$	$\frac{C}{\text{s}^{-2}}$	$\frac{\tau_{\text{R}}}{\text{s}}$	$\frac{E}{\text{s}^{-2}}$	$\frac{\tau_{\text{L}}}{\text{s}}$	$\frac{\nu_{\text{L}}}{\text{Hz}}$
Reentrant 27 °C										
1	$6.0 \cdot 10^3$		0	$5.8 \cdot 10^{10}$	$6.0 \cdot 10^{\;10}$					
2	$6.0 \cdot 10^3$		$1.6 \cdot 10^4$	$5.4 \cdot 10^{10}$	$9.6 \cdot 10^{-10}$	$4.5 \cdot 10^7$	$2.0 \cdot 10^{-8}$			
3	$6.0 \cdot 10^3$		$1.6 \cdot 10^4$	$5.4 \cdot 10^{10}$	$9.6 \cdot 10^{-10}$	$4.5 \cdot 10^7$	$2.0 \cdot 10^{-8}$	$3.0 \cdot 10^5$	$1.5 \cdot 10^{-5}$	$8.0 \cdot 10^3$
Smectic 37 °C										
1		$2.2 \cdot 10^5$	0	$5.8 \cdot 10^{10}$	$4.5 \cdot 10^{-10}$					
2		$1.5 \cdot 10^5$	$1.2 \cdot 10^4$	$5.8 \cdot 10^{10}$	$4.5 \cdot 10^{-10}$	$3.0 \cdot 10^7$	$4.0 \cdot 10^{-8}$			
3		$1.5 \cdot 10^5$	$1.2 \cdot 10^4$	$5.8 \cdot 10^{10}$	$4.5 \cdot 10^{-10}$	$3.0 \cdot 10^7$	$4.0 \cdot 10^{-8}$	$1.2 \cdot 10^5$	$2.0 \cdot 10^{-5}$	$7.0 \cdot 10^3$
Nematic 47 °C										
3	$3.5 \cdot 10^3$		$8.7 \cdot 10^3$	$5.0 \cdot 10^{10}$	$3.2 \cdot 10^{-10}$	$1.5 \cdot 10^7$	$0.8 \cdot 10^{-8}$	$2.0 \cdot 10^5$	$3.5 \cdot 10^{-5}$	$3.3 \cdot 10^3$

despite the rather dissimilar dispersion profiles, the relevant optimization criteria are the same in both cases, though they are better seen for the smectic than for the reentrant sample. The first fitting step reveals that the $T_1(\nu)$ data can be understood surprisingly well by a combination of only two contributions, namely $T_{1\text{OF}(i)}$ with zero cut-off frequency ($\tau_{\text{OF}} = 1/2\pi\nu_c = \infty$) and $T_{1\text{SD}}$ with a jumping time (τ_{SD}) of the order of 10^{-9} s. However, at very low and at medium Larmor frequencies there exist clear deviations from this simple model far outside the experimental error limits, which requires the observance of a finite OF mode parameter and refinements by one or more additional terms. A non-negligible $T_{1\text{R}}$ process has been reported previously by several field-cycling studies of nematics and smectics [19–21, 35–37]. As illustrated by the second fitting step, it's inclusion eliminates the deviations at medium values of ν, but obviously the extension cannot improve the quality of the model in the transition range to the low ν plateau, where a finite OF mode parameter τ_{OF}, i.e. a non-zero cut-off frequency, is hard to combine with the occurrence of a $T_1(\nu)$ dip: On the one hand the functions $f_{\text{OF}(i)}$ reduce the slope of the asymptotically square-root or linear dispersion profiles, whereas on the other the superimposed relaxation minimum involves an increasing slope! Our formal solution of the dilemma by taking into account a Lorentzian term $T_{1\text{L}}$ is presented in the final fitting step. It is clearly seen that the relative importance of $T_{1\text{L}}$ is somewhat smaller in the reentrant mixture than in the smectic one. In both cases, the combination with $T_{1\text{OF}}$, $T_{1\text{SD}}$, and $T_{1\text{R}}$ results in a quite satisfactory description of the experimental behaviour.

All model parameters evaluated in this way are summarized in Table 2. Note that the accuracy of the various constants differs widely, since the optimization procedure has to handle sensitive and less-sensitive analytical dependences, and because some of the constants are strongly correlated [26, 45]. Whereas $A_{(i)}$, $\tau_{\text{OF}(i)}$ and ν_{L} can be determined from the measurements almost independently of the other parameters due to their characteristic effects on the overall $T_1(\nu)$ profile, this is not possible for the amplitudes B, C, E and time constants τ_{SD}, τ_{R}, τ_{L}. As a consequence, the related contributions cannot be separated unambiguously without some additional assumptions, essentially because their dispersion occurs in similar or even overlapping frequency ranges; thus the experimental errors prevent that only one unique model combination fits to the data. In Figs. 4 and 5 the problem is seen to be twofold, since the diffusional dispersion ($T_{1\text{SD}}(\nu)$) interferes with the rotational one ($T_{1\text{R}}(\nu)$), and the collective process ($T_{1\text{OF}}(\nu)$) with the Lorentzian one ($T_{1\text{L}}(\nu)$). We restricted the number of free combinations by making $T_{1\text{SD}}$ compatible with estimations on the self-diffusion constant in comparable mesogens [47–50], and by reducing the importance of $T_{1\text{L}}$ as far as justifiable for a satisfactory optimization. These two constraints always led to a well-defined reproducible solution as illustrated by the diagrams.

3.2. *Interpretation*

The presented curve fittings clearly show on the one hand the close parallels between the proton spin relaxation in the reentrant (low-temperature) and the normal (high-temperature) nematic mesophase of the 6OCB–8OCB mixture, and on the other the strongly different behaviour in the (intermediate) smectic range. Obviously, the observed details are more complicated than assumed in the works of Dong [1–6] and Miyajima [7, 8], in particular due to the presence of two distinct kinds of order fluctuations (nematic, smectic), and due to the finding of two separate low-field relaxation processes. As a consequence, our analysis does not support the interpretation of T_1 measurements in reentrant systems described in the literature. To understand the meaning of the relaxation parameters evaluated in this paper (Table 2), let us now consider the four contributions in (2) explicitly in terms of molecular properties.

(a) Order fluctuations (OF_{nem}, OF_{sm}). The relaxation rate caused by collective molecular reorientations, and hence the related amplitudes (A_{nem}, A_{sm}) and cut-off frequencies ($\nu_{c\,nem}$, $\nu_{c\,sm}$), are of the same order of magnitude as measurements available for several non-reentrant nematic or smectic mesophases [18–22, 34–37]. This implies that the relative importance of the nematic-type fluctuations on T_1 is notably different from that of the smectic-type fluctuations (in Figs. 4 and 5, $T_{1OF\,nem}/T_{1OF\,sm} \approx 1/5$ for $\nu \to 0$), whereas the changes of the cut-off frequency or the related time constant are less evident (in Figs. 4 and 5, $\nu_{c\,nem}/\nu_{c\,sm} \approx 1/2$). Also as usual we have $A_{nem} < A_{sm}$, which essentially reflects the unlike exponents in the underlying dispersion law. Therefore it can be expected that the new results for the reentrant system are explicable by the pertinent viscoelastic and geometrical qualities defined in the Pincus-Blinc-Freed theory [27–29, 39–41, 43]. However, since at present neither the viscosities (η) nor the elastic constants (K) necessary to evaluate A_{nem} and A_{sm} are available for the 6OCB–8OCB alloy, we can only make some general estimations by means of data for the pure compounds. This reveals two remarkable aspects:

First, it follows from the negligible small temperature dependence of ν_c that also the coherence length

$$\xi \equiv \lambda_{max} = \left[\frac{2\pi}{\nu_c}\,\frac{K}{\eta}\right]^{1/2} \tag{3}$$

which measures the longest mode of collectively fluctuating molecules [40, 43, 45, 46], does not change significantly at different temperatures, since the ratio K/η of some alkylcyanobiphenyls has been reported to be approximately constant [51]. Using $\nu_{c\,nem} \cong \nu_{c\,sm} = 10^4$ Hz together with the estimations $K = 5 \cdot 10^{-12}$ N, $\eta = 5 \cdot 10^{-2}$ Pa s (nematic phase) or $K = 5 \cdot 10^{-11}$ N, $\eta = 5 \cdot 10^{-1}$ Pa s (smectic phase), respectively [52–55], (3) gives in both cases $\xi = 2.5 \cdot 10^{-7}$ m, that means about 125 molecular lengths [56, 57]. Almost the same result is obtained from the amplitude factor A_{sm} via [29, 37]

$$\xi = \frac{9}{8}\left[\frac{\mu_0}{4\pi}\right]^2 \gamma^4 \hbar^2 \,\frac{k\,\vartheta\, S^2}{4\,K\,A_{sm}}\,\frac{1}{a^6}\left[\frac{3\cos^2\varphi - 1}{2}\right]^2, \tag{4}$$

where S, a, and φ denote the relevant orientational order parameter, the spin pair separation, and the spin pair inclination relative to the molecular axis (see Table 1). If one puts $S = 0.6$, and either for the phenyl protons $a = 2.48 \cdot 10^{-10}$ m with $\varphi = 0$ or for the CH_2 protons $a = 1.79 \cdot 10^{-10}$ m with $\varphi = 90°$, then the weighted average for these protons of the two nOCB molecules, which neglects effects from the highly mobile methyl groups and from neighbouring pairs, becomes $\xi = 1.9 \cdot 10^{-7}$ m, i.e. only 25% less than from the previous estimation. This consistency between the two approaches certainly supports that our model is basically correct. Note that (3) includes the viscosity, whereas (4) does not!

Second, attention should be focused on the rather small ratio $T_{1OF\,nem}/T_{1OF\,sm}$ in the limit $\nu \to 0$, which is surprising in view of the stronger smectic dispersion law. However, considering the theoretical background of the relaxation processes, the finding $T_{1OF\,nem} < T_{1OF\,sm}$ turns out to be another support of the given interpretation: Since the derivation of $T_{1OF\,sm}$ [29] assumes a restriction of the collective mode propagation parallel to the planes of the smectic layer, whereas the propagation in the nematic phase is allowed in all three directions, the number of smectic modes is smaller than the number of nematic modes; therefore $T_{1OF\,nem}$ can become much shorter than $T_{1OF\,sm}$, provided this effect is not compensated by changes of other model parameters as e.g. the elastic constant (see Table 1). Such an increase of T_{1OF} at the nematic to smectic phase transition is known in the literature for several non-reentrant mesogens [34, 35]. It's observation in the present study at both the nematic to smectic and the reentrant nematic to smectic transition underlines the close parallels between the collective reorientations in the two nematic states, and thus corroborates our main conclusion. According to (2), the magnitude of the discontinuities depends on the Larmor frequency and numerous material parameters, most of which are not available for a quantitative evaluation. In particular, effects due to the coherence length(s) ξ introduced by (3) and (4) are hard to estimate. But one special aspect concerning the ratio $T_{1\mathrm{OF\,nem}}/T_{1\mathrm{OF\,sm}}$ with the details of Table 1 should be emphasized: The relations $A_{\mathrm{sm}} \sim 1/\xi$ and $1/T_{1\mathrm{OF\,sm}} \sim A_{\mathrm{sm}}$ do not entail a dramatic shortening of the relaxation time when the coherence length becomes small, inspite of the apparent singularity for $\xi \to 0$. Since the spectral function $f_{\mathrm{OF\,sm}}$ also includes ξ, the singularity disappears and $T_{1\mathrm{OF\,sm}}(\xi)$ runs through a minimum, where the linear dependence changes to an inverse proportional behaviour.

(b) Self-diffusion (SD). Up to now proton relaxation studies, even those which analyse the frequency dependence, have generally not succeeded to provide reliable data of the self-diffusion tensor for liquid crystals, essentially because of the difficulty to separate correctly the various processes inducing the magnetization decay. As a rule, measurements by means of the relaxation dispersion turned out almost one order of magnitude smaller than the more direct results obtained by tracer techniques or pulsed field-gradient NMR [47, 48]. The discrepancies have been attributed to the neglect or incomplete handling of the competing relaxation mechanisms, in other words to the high number of free model parameters and to the non-negligible experimental errors. In order to avoid the issue of wrong diffusion constants, we combined the fitting procedure of (2) with restrictions imposed on $T_{1\mathrm{SD}}$ by given values of the orientationally averaged self-diffusion constant $\bar{D} = D$ (suited to the isotropic approximation of $T_{1\mathrm{SD}}$), and by the Einstein relation [38]

$$d^2 = 6\,D\,\tau_{\mathrm{SD}} \tag{5}$$

between the closest spin approach d and the translational jump time τ_{SD}. In this way the low-frequency asymptote $T_{1\mathrm{SD}}(\nu \to 0)$ and the dispersion frequency $\nu_{\mathrm{SD}} \equiv 1/(2\pi\,\tau_{\mathrm{SD}})$ become correlated, i.e. in the fit they cannot be shifted independently. Written explicitly with the notation of Table 1 and τ_{SD} substituded by $d^2/(6\,D)$, we have

$$\frac{1}{T_1(0)} = \left[\frac{\mu_0}{4\pi}\right]^2 \frac{0.4\,\pi\,\gamma^4\,\hbar^2\,N}{\mathrm{d}D} \tag{6}$$

and

$$\tau_{\mathrm{SD}} = \frac{3}{\pi}\,\frac{D}{d^2}\,, \tag{7}$$

which is a most convenient tool to control the value of the self-diffusion constant in the course of the various optimization steps.

Since diffusion studies of oxycyanobiphenyls could not be found in the literature and our intended field-gradient field-cycling measurements [48] need some instrumental modifications, we resorted to results reported by Hara et al. [49] for 4′-n-pentyl-4-cyanobiphenyl (5 CB), and looked for a solution with D near $10^{-11}\ \mathrm{m^2/s}$ at room temperature. The best model fits under such a constraint are illustrated in Figs. 4 and 5. Using the observed asymptotes $T_{1\mathrm{SD}}(0)$, the proton density $N = 4.79 \cdot 10^{28}\ \mathrm{m^{-2}}$ calculated from the molecular weight of the 6 OCB – 8 OCB mixture with a mass density $\varrho = 1\ \mathrm{g/cm^3}$, and $D = 1.3 \cdot 10^{-11}$, $1.5 \cdot 10^{-11}$, $2.8 \cdot 10^{-11}\ \mathrm{m^2/s}$ for 27, 37, 47 °C, respectively, (6) yields $d = 2.3 \cdot 10^{-10}$ m, if the temperature effects by ϱ are neglected. This is a surprisingly small (average) intermolecular proton approach in view of the molecular width of about $6 \cdot 10^{-10}$ m; it points out that some details of the model are not yet understood satisfactorily. The steadiness of $D(\vartheta)$ is in accordance with Krüger's extensive works on self-diffusion in liquid crystals, which generally do not reveal a significant discontinuity of D (or the components of the diffusion tensor) at mesophase transitions. However, it must be admitted that model fits with considerably larger and discontinuous diffusion constants could not be excluded, and probably will become important as soon as more exact data are available. In the case of 4-methoxybenzylidene-4′-butylaniline (MBBA), where the optical investigations of Hara [49] can be compared with pulsed field-gradient NMR studies [48], there exist dramatic discrepancies; the self-diffusion observed by the NMR method is faster by approximately a factor of ten!

(c) Rotations (R). Because of the difficult separation from collective fluctuations, the effect of individual molecular rotations on the nuclear spin relaxation in liquid crystals is only poorly understood. It is undisputed in the literature that rotations of whole molecules as well as intramolecular reorientations with typical time constants of the order of 10^{-8} s contribute to both the proton and deuteron spin relaxation of alkylcyanobiphenyls [22, 58–60]. This time scale has also been found in the low-frequency dielectric absorption spectrum [61]. But most details of the anisotropic rotational diffusion, e.g. the distinction between small-step and jump rotations, the significance of the ordering potential, or the interference with collective mechanisms, could not be analysed convincingly by NMR methods [41–43, 62–64]. Although field-cycling studies considerably improved the disentanglement of the basic effects, the present high-field limitations still strongly hinder to find reliable answers to such more special questions [17–22, 35–37]. Therefore, and also on account of the uncertain self-diffusion term for the oxycyanobiphenyls, we tried model fits only with the simple Bloembergen-Purcell-Pound (BPP) ansatz [38], which neglects all effects due to the molecular anisotropy. The two optimized parameters for a BPP contribution, namely the rotational time constant τ_R and the amplitude factor C, are given in Table 2. It is seen that on the one hand τ_R does not steadily decrease with growing temperature at the phase transitions, the longest time appears in the intermediate smectic state ($\tau_R = 4.0 \cdot 10^{-8}$ s at 37 °C). On the other hand, C decreases continuously, so that according to [38]

$$C = \frac{9}{8}\left[\frac{\mu_0}{4\pi}\right]^2 \gamma^2 \hbar^2 \frac{4}{15 b^6} \tag{8}$$

the fittings imply a rather strong variation of the effective intramolecular proton pair separation b (from $3.95 \cdot 10^{-10}$ m at 27 °C to $4.74 \cdot 10^{-10}$ m at 47 °C). Obviously, this change is too large to be described correctly by (8), i.e. without including the orientational distribution of pair axes. Making use of Woessner's formalism [32, 33] for relaxation by anisotropic rotations, the temperature dependence of C may be partly attributed to different inclinations of individual spin pair axes relative to the external magnetic field. However, the presently available experimental results, in particular the lack of deuteron measurements, do not yet allow a clear separation of the involved positional and angular coordinates.

(d) Lorentzian Term (L). The most unusual feature of the relaxation dispersion profiles is the occurrence of a rather narrow $T_1(\nu)$ minimum ("dip") near $\nu \cong 10^4$ Hz for the 6OCB–8OCB mixture. Since the effect was not found in the pure compounds, we originally looked for an explanation based on the reentrant behaviour. Note that the absence of the dip for the pure components excludes instrumental errors as a potential origin. Nevertheless, the assumption of an additional special reorientation process in the mixture could not be maintained after extensive controls [26], and there are many reasons to prefer another, more general interpretation: As first observed and discussed by Kimmich et al. [16, 65, 66], the quadrupolar nuclei of a spin system like nitrogen may dramatically enhance the proton relaxation rate, if in a field-cycling experiment the proton Larmor frequency

$$\nu_L = \gamma B/(2\pi) \tag{9a}$$

coincides with one of the quadrupole transition frequencies [67]

$$\nu_{Q\pm} = \frac{3}{2\pi} K_Q (1 \pm \eta_Q/3), \tag{9b}$$

$$\nu_{Q_0} = \frac{1}{\pi} K_Q \eta_Q \tag{9c}$$

of the nitrogen spins. Accordingly, there exists either a single ($\eta_Q = 0$) or a triple ($\eta_Q \neq 0$) resonance at Zeeman fields B determined by the effective quadrupolar coupling constant K_Q in conjunction with the electric field gradient asymmetry η_Q of the quadrupole site, and by the magnetogyric ratio γ of the magnetic dipole. Such level crossings have long been overlooked for liquid crystals, because in this case they are harder to detect than in the materials studied by Kimmich. Though their effects on $T_1(\nu)$ could be verified already in 1986 [17] for a special deuterated liquid crystal, a systematic investigation of mesogenic molecules with nitrogen atoms has been reported only recently [68]. The results obtained for some azoxybenzenes and cyanobiphenyls show that the frequencies ν_0, ν_+, and ν_- are distributed typically between 1 kHz and 5 MHz, and reveal a strong dependence on the molecular structure, the position of the nitrogen, the kind of mesophase, and the sample temperature. As a rule, the width of the resonances turned out to be of the order of 10 kHz to 50 kHz, but some dips were much sharper and almost undetectable. In view of these findings, we suggest to attribute the $T_1(\nu)$ minima seen in Figs. 1 and 2 to the low quadrupole transition frequency ν_0 of the involved oxycyano group, averaged over the two types of molecules in the mixture.

At the moment it is not quite clear why such resonances have not been confirmed previously in all relaxation dispersion studies of mesogens with nitrogen atoms, in particular why they could not be resolved in the extensive works on phenylcyclohexanes [22]. Also it is difficult to understand that the high-frequency dips ν_+ and ν_- are absent in our new measurements on the reentrant system. However, realizing the experimental problems to find the level crossings if the width is very sharp, say less than 1 kHz, their non-appearance in the $T_1(\nu)$ profiles probably merely indicates that the minimum adjustable field steps of the spectrometer are too coarse. In the important frequency range from about 0.2 MHz to 2 MHz, the presently used digitization limits the finest step interval to 2 kHz, which obviously is insufficient. By searching for the level crossings through temperature variation at a fixed field, one of the (up to four) expected high quadrupole transition resonances developed at 1.6 MHz in the smectic phase of the 6OCB–8OCB alloy [26].

Without knowledge of the complete triplet predicted by (9), it is not possible to separate the underlying coupling parameters (K_Q, η_Q) for a quantitative comparison with normal nematic and smectic liquid crystals [68]. Nevertheless, already the available data reveal two essential aspects about the distinctions: First, the effective proton-nitrogen coupling, i.e. the relaxation rate exchange, is stronger in the mixture than in the pure compounds. We attribute this to the wellknown property of molecular dimerization [9]. Second, the dip frequency has almost the same value for the reentrant and smectic phase, inspite of the large temperature shift. This supports the conclusions drawn from the order fluctuation term, namely that the slow collective motions in the two mesophases are basically different.

Acknowledgements

The authors thank Dipl.-Phys. R. Krieg, Dr. D. Pusiol, Dipl.-Phys. A. Rudnicki, and Mr. P. Sebastião for their contributions to this work. Thanks are also due to the Deutsche Forschungsgemeinschaft for financial support.

[1] R. Y. Dong, J. Chem. Phys. **75,** 2621 (1981).
[2] R. Y. Dong, Mol. Cryst. Liq. Cryst. **64,** 205 (1981).
[3] R. Y. Dong, J. Chem. Phys. **76,** 5659 (1982).
[4] R. Y. Dong, Mol. Cryst. Liq. Cryst. **92,** 251 (1984).
[5] R. Y. Dong, J. S. Lewis, E. Tomchuk, and E. Bock, Mol. Cryst. Liq. Cryst. **122,** 35 (1985).
[6] R. Y. Dong, G. M. Richards, J. S. Lewis, E. Tomchuk, and E. Bock, Mol. Cryst. Liq. Cryst. **144,** 33 (1987).
[7] S. Miyajima, K. Akaba, and T. Chiba, Sol. State Commun. **49,** 675 (1984).
[8] S. Miyajima and T. Chiba, J. Phys. Soc. Japan **57,** 2550 (1988).
[9] P. E. Cladis, Mol. Cryst. Liq. Cryst. **165,** 85 (1988).
[10] S. Chandrasekhar, Mol. Cryst. Liq. Cryst. **124,** 1 (1985).
[11] L. Longa and W. H. de Jeu, Phys. Rev. **A 26,** 1632 (1982).
[12] D. Guillon and A. Skoulios, J. Phys. France **45,** 607 (1984).
[13] J. O. Indekeu and A. N. Berker, J. Phys. France **49,** 353 (1988).
[14] A. J. Leadbetter, J. C. Frost, J. P. Gaughan, G. W. Gray, and A. Mosley, J. Phys. France **40,** 375 (1979).
[15] P. E. Cladis, D. Guillon, F. R. Bouchet, and P. L. Finn, Phys. Rev. **A 23,** 2594 (1981).
[16] R. Kimmich, Bull. Magn. Res. **1,** 195 (1980).
[17] F. Noack, Progr. Nucl. Magn. Res. Spectrosc. **18,** 171 (1986).
[18] W. Wölfel, F. Noack, and M. Stohrer, Z. Naturforsch. **30a,** 437 (1975).
[19] V. Graf, F. Noack, and M. Stohrer, Z. Naturforsch. **32a,** 61 (1977).
[20] R. Blinc, M. Vilfan, M. Luzar, J. Seliger, and V. Žagar, J. Chem. Phys. **68,** 303 (1978).
[21] G. Nagel, W. Wölfel, and F. Noack, Israel J. Chem. **23,** 380 (1983).
[22] F. Noack, M. Notter, and W. Weiß, Liq. Cryst. **3,** 907 (1988).
[23] M. Stohrer and F. Noack,. J. Chem. Phys. **67,** 3729 (1977).
[24] E. Rommel, K. Mischker, G. Osswald, K. H. Schweikert, and F. Noack, J. Magn. Reson. **70,** 219 (1986).
[25] K. H. Schweikert, R. Krieg, and F. Noack, J. Magn. Reson. **78,** 77 (1988).
[26] a) K. H. Schweikert, Diplomarbeit, Universität Stuttgart 1985. – b) A. Rudnicki, Diplomarbeit, Universität Stuttgart 1989.
[27] P. Pincus, Solid State Commun. **7,** 415 (1969).
[28] R. Blinc,. D. L. Hogenboom, D. E. O'Reilly, and E. M. Peterson, Phys. Rev. Lett. **23,** 969 (1969).
[29] R. Blinc, M. Luzar, M. Vilfan, and M. Burgar, J. Chem. Phys. **63,** 3445 (1975).
[30] H. C. Torrey, Phys. Rev. **92,** 962 (1953).
[31] H. Pfeifer, Ann. Phys. Leipzig **8,** 1 (1961).
[32] D. E. Woessner, J. Chem. Phys. **37,** 647 (1962).
[33] G. Lipari and A. Szabo, J. Amer. Chem. Soc. **104,** 4546 (1982).
[34] G. J. Krüger, H. Spiesecke, R. van Steenwinkel, and F. Noack, Mol. Cryst. Liq. Cryst. **40,** 103 (1977).
[35] Th. Mugele, V. Graf, W. Wölfel, and F. Noack, Z. Naturforsch. **35a,** 924 (1980).
[36] W. Kühner, E. Rommel, F. Noack, and P. Meier, Z. Naturforsch. **42a,** 127 (1987).
[37] E. Rommel, F. Noack, P. Meier, and G. Kothe, J. Phys. Chem. **92,** 2981 (1988).
[38] A. Abragam, The Principles of Nuclear Magnetism, Clarendon, Oxford 1962.
[39] J. W. Doane and D. L. Johnson, Chem. Phys. Lett. **6,** 291 (1970).
[40] I. Zupančič, V. Žagar, M. Rožmarin, I. Levstik, F. Kogovšec, and R. Blinc, Solid State Commun. **18,** 1591 (1976).
[41] P. Ukleja, J. Pirs, and J. W. Doane, Phys. Rev. A **14,** 414 (1976).

[42] P. L. Nordio and U. Segre, J. Magn. Reson. **27,** 465 (1977).

[43] J. Freed, J. Chem. Phys. **66,** 4183 (1977).

[44] S. Žumer and M. Vilfan, Phys. Rev. **A 17,** 424 (1978).

[45] V. Graf, Thesis, Universität Stuttgart 1980.

[46] M. Vilfan, M. Kogoj, and R. Blinc, J. Chem. Phys. **86,** 1055 (1987).

[47] G. J. Krüger, Phys. Rep. **82,** 229 (1982).

[48] F. Noack, Mol. Cryst. Liq. Cryst. **113,** 247 (1984).

[49] M. Hara, S. Ichikawa, H. Takezoe, and A. Fukuda, Jap. J. Appl. Phys. **23,** 1420 (1984).

[50] H. Takezoe, M. Hara, S. Ichikawa, and A. Fukuda, Mol. Cryst. Liq. Cryst. **122,** 169 (1985).

[51] J. Hirakata, G. Chen, T. Toyooka, S. Kawamoto, H. Takezoe, and A. Fukuda, Jap. J. Appl. Phys. **25,** L 607 (1986).

[52] P. P. Karat and N. V. Madhusudana, Mol. Cryst. Liq. Cryst. **36,** 51 (1976); Mol. Cryst. Liq. Cryst. **40,** 239 (1977).

[53] S. Bhattacharya and S. V. Letcher, Phys. Rev. Lett. **44,** 414 (1980).

[54] M. Hara, J. Hirakata, T. Toyooka, H. Takezoe, and A. Fukuda, Mol. Cryst. Liq. Cryst. **122,** 161 (1985).

[55] S. W. Morris, P. Palffy-Muhoray, and D. A. Balzarini, Mol. Cryst. Liq. Cryst. **139,** 263 (1986).

[56] A. J. Leadbetter, R. M. Richardson, and C. N. Collings, J. Phys. Coll. **36,** C 1-37 (1975).

[57] B. Bhattacharjee, S. Paul, and R. Paul, Mol. Cryst. Liq. Cryst. **89,** 181 (1982).

[58] P. R. Luyten, R. R. Vold, and R. L. Vold, J. Phys. Chem. **89,** 545 (1985).

[59] P. A. Beckmann, J. W. Emsley, G. R. Luckhurst, and D. L. Turner, Mol. Phys. **59,** 97 (1986).

[60] J. S. Lewis, E. Tomchuk, H. M. Hutton, and E. Bock, Can. J. Phys. **65,** 115 (1987).

[61] T. K. Bose, B. Campbell, S. Yagihara, and J. Thoen, Phys. Rev. **A 36,** 5767 (1987).

[62] T. E. Faber, Proc. Roy. Soc. Lond. **A 353,** 277 (1977).

[63] R. R. Vold and R. L. Vold, J. Chem. Phys. **88,** 1443 (1988); J. Chem. Phys. **88,** 4655 (1988).

[64] R. Y. Dong, J. Chem. Phys. **88,** 3962 (1988).

[65] F. Winter and R. Kimmich, Mol.- Phys. **45,** 33 (1982).

[66] F. Winter and R. Kimmich, Biochim. Biophys. Acta **719,** 292 (1982).

[67] T. P. Das and E. L. Hahn, Nuclear Quadrupole Resonance Spectroscopy, Academic Press, New York 1958.

[68] D. Pusiol and F. Noack, Liq. Cryst. **4,** in press (1989).